

LEVEL

12  
MC

A08\*BI

AD A091983

HgCdTe FABRICATION USING DIRECTED ENERGY TECHNIQUES

DTIC  
EXTRACTE  
NOV 7 1980  
C

ROBERT WOLFSON  
(617) 275-6000 EXT. 256

ANTON GREENWALD  
(617) 275-6000 EXT. 238

SEPTEMBER 1980  
Semiannual Technical Report

THIS RESEARCH WAS SPONSORED BY THE DEFENSE ADVANCED  
RESEARCH PROJECTS AGENCY UNDER ARPA ORDER NO. 3800  
CONTRACT NO: MDA 903-79-C-0434  
MONITORED BY: DR. R.A. REYNOLDS, DARPA/MSO  
1400 WILSON BLVD, ARLINGTON, VA 22209

EFFECTIVE DATE: 16 AUGUST 1979  
EXPIRATION DATE: 30 JUNE 1981  
PERIOD COVERING: 1 MARCH THROUGH 31 AUGUST 1980

Approved for Public Release: distribution unlimited

DOC FILE COPY



spire

80 10 31 050

The views and conclusions contained in this document are those of the author and should not be interpreted as necessarily representing the official policies, either expressed or implied, of the Defense Advanced Research Projects Agency or the United States Government.



20. graphoepitaxial growth of a thin crystalline film, and for pulse annealing high-dose implants in CdTe. This new technology should result in larger, more uniform crystals of HgCdTe than are currently available (and unsuitable) for the proposed application.

Results to date have demonstrated that single-crystal CdTe films up to 17  $\mu\text{m}$  thick can be deposited on mica, and that CdTe and HgCdTe can be pulse processed without damaging the surface. Initial nonstoichiometric evaporations have been corrected. Thin film, single-crystal HgCdTe is expected to be available by the next reporting period.

DISTRIBUTION

Director  
Defense Advanced Research Projects Agency  
Arlington, VA 22209

Attn: Program Management (2)  
Attn: Dr. Richard A. Reynolds (1)  
Attn: Dr. Sven Roosilid (1)

Defense Documentation Center (12)  
Cameron Station  
Alexandria, VA 22314

Spire Corporation Distribution

A. Greenwald (1)  
R. Little (1)  
R. Wolfson (1)  
Files Original + (6)

NERC Distribution

T. Wong (1)  
J. Miles (1)  
Files (1)

Accession For	
NTIS GRA&I	<input checked="" type="checkbox"/>
DTIC TAB	<input type="checkbox"/>
Unannounced	<input type="checkbox"/>
Justification	
By _____	
Distribution/	
Availability Codes	
Avail and/or	
Dist	Special
A	

## FOREWORD

The work reported in this document was performed in part at Spire Corporation, Bedford, Massachusetts, and in part at New England Research Center, Inc., Sudbury, Massachusetts, under contract MDA 903-79-C-0434, DARPA order number 3800. The contract monitor is Dr. R.A. Reynolds.

The program manager at Spire is Dr. Robert Wolfson. The principal investigator at Spire is Dr. Anton Greenwald, who is in charge of pulsed electron beam processing and ion implantation studies. The program manager at NERC is Dr. Ted Wong. The principal investigator at NERC is Mr. John Miles, who is in charge of the epitaxial deposition and vapor exchange processes.

The report of the main subcontractor, NERC, is included herein.

## TABLE OF CONTENTS

<u>Section</u>	<u>Page</u>
SUMMARY . . . . .	1-1
1 INTRODUCTION . . . . .	1-2
1.1 Purpose . . . . .	1-2
1.2 Technical Considerations . . . . .	1-2
1.3 General Methods . . . . .	1-2
1.4 Technical Results and Conclusions . . . . .	1-3
1.5 Implications for Future Research . . . . .	1-3
1.6 Significant Hardware Development . . . . .	1-3
2 TECHNICAL INFORMATION . . . . .	2-1
2.1 Directed Energy Processing Assessment (Taks 1) . . . . .	2-1
2.2 Deposition of Single-Crystal CdTe Films (Task 2) . . . . .	2-1
2.2.1 Objective . . . . .	2-1
2.2.2 Hot Wall Furnace Apparatus . . . . .	2-1
2.2.3 Films Deposited on Mica . . . . .	2-6
2.2.4 Characterization of Single-Crystal Films . . . . .	2-7
2.2.5 Films Deposited on Other Substrates . . . . .	2-8
2.3 Pulsed Electron Beam Processing of CdTe Films (Task 2) . . . . .	2-13
2.3.1 Objective . . . . .	2-13
2.3.2 Equipment . . . . .	2-13
2.3.3 Heteroepitaxy Results . . . . .	2-18
2.3.4 Graphoepitaxy Results . . . . .	2-20
2.4 Vapor Exchange of CdTe to Form HgCdTe (Task 4) . . . . .	2-23
2.4.1 Objective . . . . .	2-23
2.4.2 Process Considerations . . . . .	2-23
2.4.3 Initial Results . . . . .	2-25
2.4.4 Film Characterization . . . . .	2-26
2.5 Modification of CdTe by Ion Implantation (Task 4) . . . . .	2-26
2.5.1 Objective . . . . .	2-26
2.5.2 Implantation and Pulse Annealing Results . . . . .	2-26
2.5.3 Analysis of High-Dose Implantation of Hg into CdTe . . . . .	2-31
2.5.4 Evaporation and Pulse Diffusion Results . . . . .	2-33
3 FUTURE PLANS . . . . .	3-1
3.1 Deposition and Pulsed Epitaxy . . . . .	3-1
3.2 Evaporation and Cascade Implantation . . . . .	3-1
3.3 Analysis . . . . .	3-1
REFERENCES	

## LIST OF FIGURES

<u>Figure</u>		<u>Page</u>
1	Initial design of hot wall furnace (at NERC) for evaporation of CdTe . . . . .	2-2
2	Redesigned hot wall furnace with enclosed source (at NERC) for evaporation of CdTe . . . . .	2-3
3	Calibration curve of the hot wall furnace: source temperature $T_s$ versus voltage $V_s$ applied to heater . . . . .	2-4
4	Calibration curve of the hot wall furnace: temperature difference between source and substrate $T_s - T_t$ as a function of the difference in voltage $V_s - V_t$ applied to heater coils . . . . .	2-5
5	Back-reflection Laue pattern from CdTe film on muscovite mica (specimen M81) . . . . .	2-9
6	Electron energy spectrum of beam used to process CdTe . . . . .	2-14
7	Deposition profile of electron beam in CdTe using the energy spectrum of figure 6 at a $45^\circ$ angle of incidence . . . . .	2-15
8	Heated sample stage for pulsed electron beam apparatus . . . . .	2-16
9	Cryogenic cooled sample stage for pulsed electron beam apparatus . . . . .	2-17
10	CdTe films on mica pulsed electron beam treated in 5mm x 5mm regions . . . . .	2-19
11	Schematic of graphoepitaxy process . . . . .	2-21
12	Graphoepitaxy experiment . . . . .	2-22
13	Schematic of vapor exchange apparatus at (NERC) . . . . .	2-24
14	Infrared transmission spectrum of CdTe film enriched in Hg by vapor exchange (specimen Si 39) . . . . .	2-27
15	IMMA depth profiles of Cd and Hg in ion implanted CdTe . . . . .	2-30
16	Concentration $x$ of $Hg_{1-x}Cd_xTe$ as a function of sputtering yield for $Hg^+$ implanted into CdTe . . . . .	2-34

## SUMMARY

The goal of this research is to produce large-area, single-crystal HgCdTe material for infrared detectors. The approach is (1) to evaporate CdTe films onto insulating substrates for epitaxial crystal growth; (2) to heat the film with a pulsed, directed energy beam to reduce defect concentration; and (3) to convert the material to HgCdTe by either vapor-exchange or ion implantation of mercury.

Twinned single-crystal films of CdTe, 17 microns thick, have been deposited on mica substrates. Better crystal structure is expected for future depositions on sapphire. Pulsed electron beams have been used to process films on mica, sapphire, and silicon. Pulsed melting without the loss of stoichiometry and with crystal regrowth have proved feasible. Analysis is continuing.

The apparatus for vapor exchange has just been completed. Initial experiments on polycrystalline films have shown the feasibility of the process. Work with better samples is just starting. Ion implantation of Hg into CdTe bulk single-crystal wafers led to excessive sputtering at ion energies of 50 keV. At lower energies, 5 keV, the correct atomic composition could be achieved by implantation, but only in a very thin, submicron layer. Greater Hg concentrations were achieved by evaporation onto a liquid nitrogen cooled substrate, followed by pulsed electron beam heating.

This program is currently on schedule. Thin-film HgCdTe should be available by the next reporting period (6 months).

## SECTION 1 INTRODUCTION

### 1.1 PURPOSE

The overall purpose of this research is to produce large-area, single-crystal HgCdTe material for infrared detectors.

### 1.2 TECHNICAL CONSIDERATIONS

The  $\text{Hg}_{1-x}\text{Cd}_x\text{Te}$  mixed-crystal system has become the leading intrinsic infrared detector material because of its continuously variable energy gap and its inherently high operating temperature. The compositions of greatest interest are near  $x=0.2$ , which corresponds to the important 8-14  $\mu\text{m}$  atmospheric transmission window. Conventional growth techniques, however, are not capable of meeting the requirements for future mosaic focal-plane applications: viz., uniformity better than 0.003 in composition, minimal vertical band-gap gradients, near-intrinsic purity, freedom from residual stresses and surface defects, size greater than 2 inches, and large-scale production capability. Therefore, a new approach to HgCdTe single-crystal production is needed which will satisfy these several constraints.

### 1.3 GENERAL METHODS

The approach taken is to vapor deposit CdTe films on foreign substrates; to crystallize the films, if necessary, by pulsed electron beam heating; and then to convert the CdTe to single-crystal HgCdTe either by the vapor exchange method or by ion implantation of Hg and Te followed by pulsed electron beam induced recrystallization. Single-crystal films will be obtained by heteroepitaxy or graphoepitaxy, the former by deposition on suitable single-crystal substrates, and the latter by the melting and crystallization of films on substrate surfaces with artificial relief patterns. Uniformity is assured because the deposition, conversion, and pulsed electron beam processes are inherently uniform. Vertical gradients are avoided by the use of thin films, as are also residual stresses and undesirable surface morphology. Since the chief potential source of contamination is the substrate, purity can be maintained by exercising normal precautions. Finally, this combined use of vapor transport and pulsed electron beam technologies imposes no limitations upon crystal area; to the contrary, the approach is admirably suited to scale-up for the high-volume production of large-area HgCdTe detector material.

#### 1.4 TECHNICAL RESULTS AND CONCLUSIONS

CdTe films, from 0.5 to over 20 micron thick, were deposited on mica, sapphire, silicon, and oxidized silicon; some of the silicon substrates had been texture-etched to produce a pattern for graphoepitaxy of the thin films. The hot wall vapor deposition apparatus initially deposited non-stoichiometric polycrystalline films. The imperfect structure and composition were retained after pulse processing with an electron beam, but surface roughness was reduced. The apparatus has since been modified, and a 17.8 micron single-crystal film of CdTe was deposited on a thick mica substrate. Samples of the better films have been pulse processed but not yet analyzed.

The vapor-exchange apparatus for converting thin-film CdTe to HgCdTe has been completed. Initial tests with polycrystalline CdTe films have shown the feasibility of growing epitaxial HgCdTe on thin-film CdTe and obtaining uniform composition through diffusion. Experiments will continue as single-crystal thin films become available. Ion implantation of bulk CdTe with Hg is limited by a sputtering coefficient in excess of 1000 at an ion energy of 50 keV. Only very thin, submicron films of CdTe could be converted to HgCdTe by this technique. An alternate method, evaporation of Hg onto a cooled CdTe substrate followed by in situ pulse heating, resulted in 40 atomic percent Hg films which remained stable when heated to room temperatures.

#### 1.5 IMPLICATIONS FOR FUTURE RESEARCH

The results obtained to date confirm the validity of the general approach. Research to improve the observed single-crystal film quality will continue using different substrates and pulse processing. The conversion of CdTe films into HgCdTe by vapor exchange, or by evaporation of Hg and implantation of Te (or vice versa) with pulse processing, will be standard during the next 6 months.

#### 1.6 SIGNIFICANT HARDWARE DEVELOPMENT

The apparatus for vapor-exchange of CdTe to  $\text{Hg}_{1-x}\text{Cd}_x\text{Te}$  was built at NERC. The initial substrate and film is supported between two ampoules in a sealed volume with a source of HgTe and a precise, excess amount of Hg. This is placed in a furnace at a constant temperature for a prolonged period of time (1 week) to form the final film. Optimization of the process will improve the design.

## SECTION 2

### TECHNICAL INFORMATION

#### 2.1 DIRECTED ENERGY PROCESSING ASSESSMENT (TASK 1)

This task has been completed, as reported in the first semiannual report.

#### 2.2 DEPOSITION OF SINGLE-CRYSTAL CdTe FILMS (TASK 2)

##### 2.2.1 Objective

The objective of this part of the program, performed at NERC, is to deposit from the vapor phase epitaxial films of CdTe on crystalline substrates such as mica, sapphire, and quartz. This task involved the construction of a suitable furnace for physical vapor deposition (PVD), experimental determination of optimum deposition parameters (which might vary with the choice of substrate), and characterization of the films as to composition and crystal structure.

##### 2.2.2 Hot Wall Furnace Apparatus

The initial design of the hot wall furnace described in our first semiannual report<sup>(1)</sup> is shown schematically in Figure 1. Analysis of the initial films deposited suggested that this design was not operating near equilibrium conditions. It was judged that the vapor pressures of Cd and Te<sub>2</sub> were incorrect because the region between the source and substrate was not sufficiently enclosed. The new furnace design is shown in Figure 2. Epitaxial films were deposited on mica with the modifications shown.

After the hot wall apparatus was redesigned and set up, calibration experiments were performed to determine the correlation between the temperatures of the source and substrate and the voltage (or current) applied to the furnace heater coils. The results of these tests are given in Figures 3 and 4. The curve in Figure 3, source temperature as a function of applied voltage, is typical for electrically heated systems with heat losses dominated by thermal conductance and radiation. The measured temperature difference between the source and substrate ( $T_S - T_T$ ) is given as a function of the applied voltage difference ( $U_S - U_T$ ) in Figure 4. Here the subscript S denotes source and T substrate. The linear dependence of ( $T_S - T_T$ ) on ( $U_S - U_T$ ) implies that only a small portion of the energy was lost through radiation between the two furnaces. For calibration purposes, the temperature-applied voltage data were fit to an empirical expression:

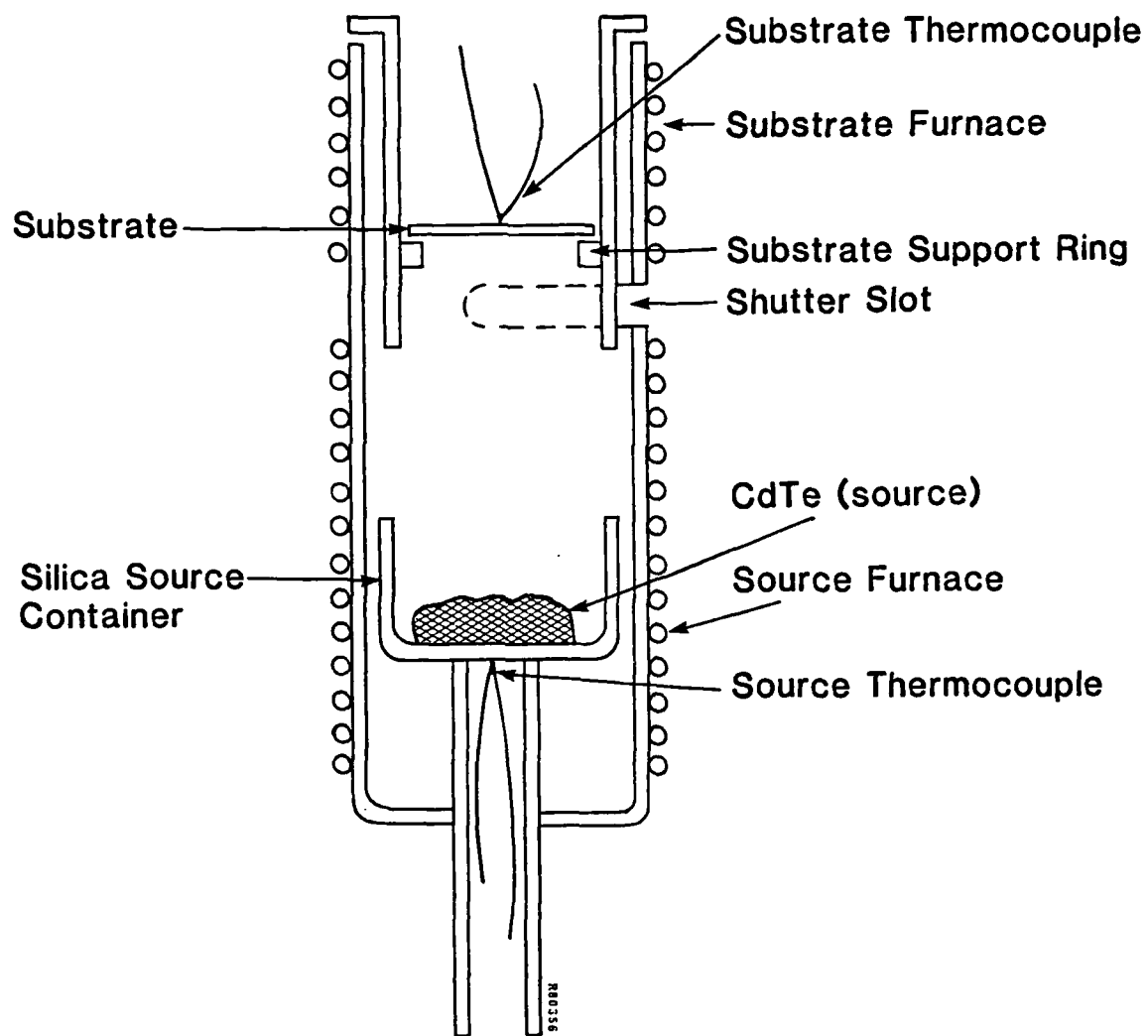


FIGURE 1. Initial design of hot wall furnace (at NERC) for evaporation of CdTe.

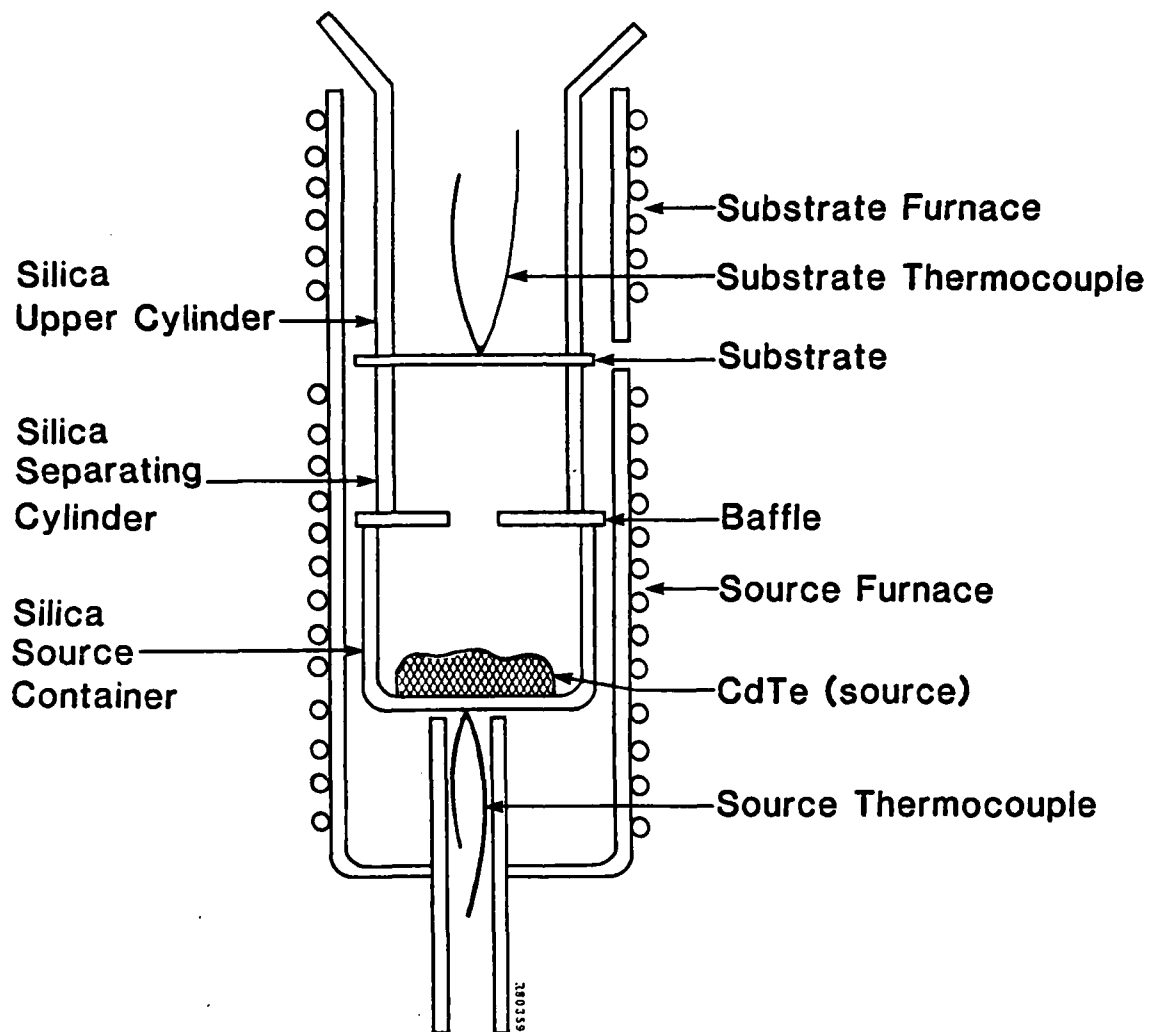


FIGURE 2. Redesigned hot wall furnace with enclosed source (at NERC) for evaporation of CdTe.

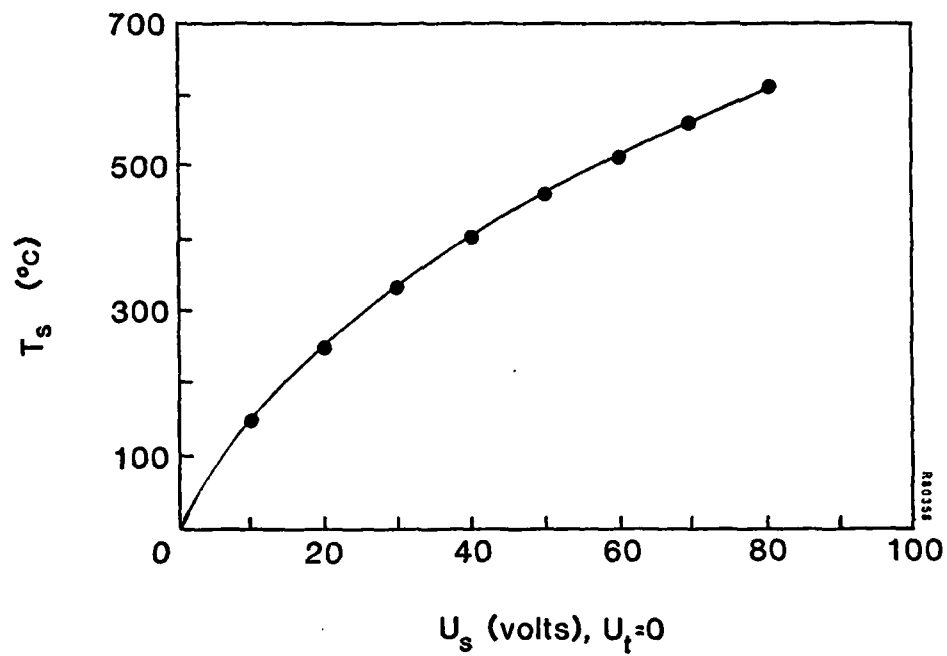


FIGURE 3. Calibration curve of the hot wall furnace: source temperature  $T_s$  versus voltage  $V_s$  applied to heater.

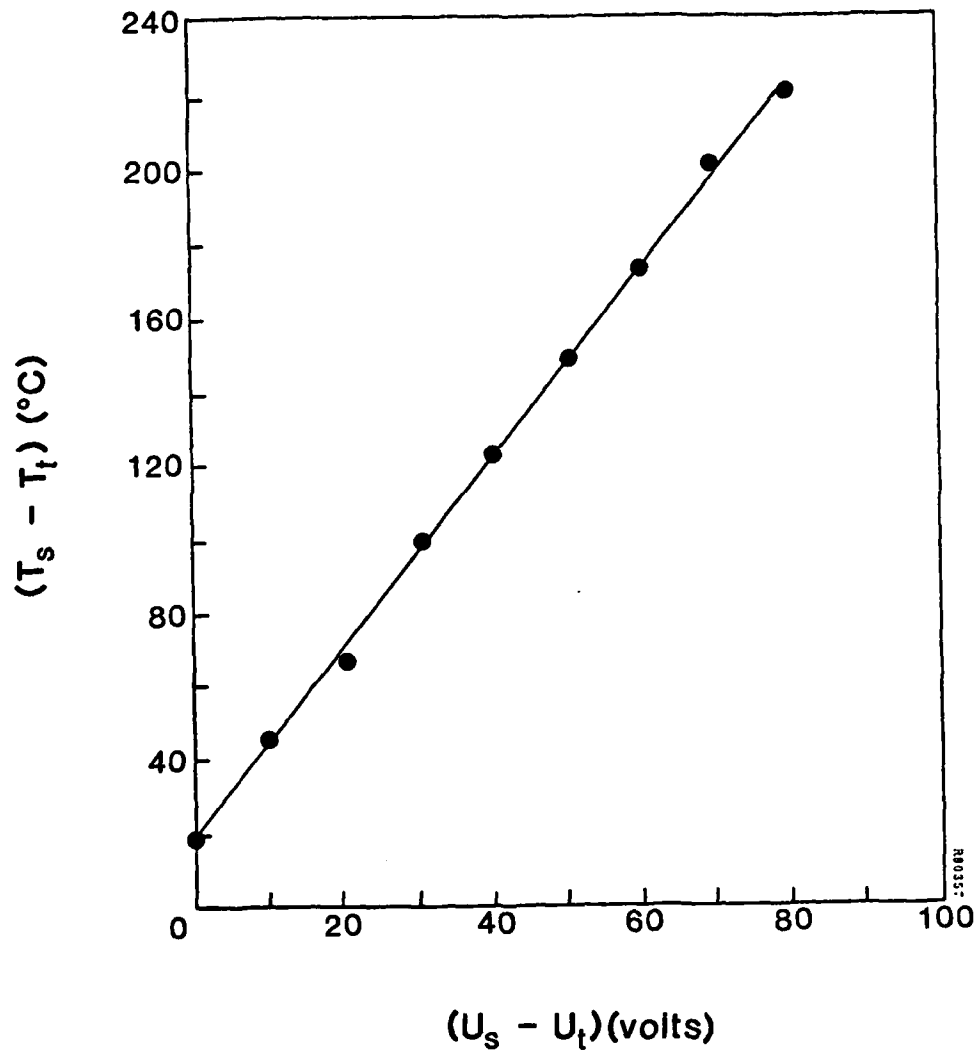


FIGURE 4. Calibration curve of the hot wall furnace: temperature difference between source and substrate  $T_s - T_t$  as a function of the difference in voltage  $V_s - V_t$  applied to heater coils.

$$T_S = a U_S^b + c U_T / U_S + d$$

where  $T_S$  = temperature of source in  $^{\circ}\text{C}$

$U_S$  = voltage applied to heater at source

$U_T$  = voltage applied to heater at substrate

a, b, c, d = constants to be determined

### 2.2.3 Films Deposited on Mica

Mica was chosen as a substrate for CdTe deposition because it cleaves readily to give a clean surface and because it has the correct crystal symmetry (hexagonal) on the surface to induce single crystal growth of the CdTe.

Previously reported results<sup>(2-7)</sup> for CdTe deposition on mica show that both sphalerite and wurtzite structures were grown for substrate temperatures  $T_T$  between 20 and 380 $^{\circ}\text{C}$ . At low temperatures the films were fine-grained and randomly oriented whereas at higher temperatures they grew epitaxially.<sup>(6)</sup> Single-crystal films were reported<sup>(8)</sup> for  $270 < T_T < 550^{\circ}\text{C}$ , with quasi-equilibrium growth conditions. "Layers with large islands of perfect structure (up to  $10^2$  grains/cm $^2$ )" were reported with a degree of supersaturation.<sup>(7)</sup>

In this program, mica was chosen as the initial substrate to investigate the influence of  $T_S$ ,  $T_T$ , and  $P/P_O$  on the deposition of CdTe. Here,  $T_S$  is the source temperature,  $T_T$  is the temperature of the substrate,  $P$  is the partial pressure of a component (Cd or Te), and  $P_O$  is its equilibrium partial pressure at  $T_T$ . NERC conducted 22 evaporation-deposition runs on freshly cleaved mica substrates. Nine of these tests were successful whereas the other 13 had some problems during deposition. Large variations in the rate of deposition and the thickness of the deposited films were observed, even when the deposition parameters were held constant. X-ray analysis showed that all of these as-grown films were fine-grained polycrystalline CdTe. These results were attributed partly to the nature of the substrate, since the high thermal resistivity and structure of mica could cause large differences in the actual deposition conditions. The other possible cause for the unpredictability was nonequilibrium conditions inside the hot wall apparatus.

Experiments with other substrate materials (Section 2.2.5) indicated that the use of mica was not the primary cause of the variability. Therefore, the hot wall apparatus was redesigned to minimize possible deviations from equilibrium (Section 2.2.2). In

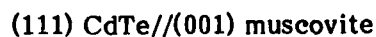
addition, thicker mica substrates were used in order to preclude flexure. Subsequent runs successfully deposited epitaxial films of CdTe up to 17 micron thick on mica. The films were approximately  $5 \text{ cm}^2$  in area. Reproducibility has been achieved in the deposition of material.

#### 2.2.4 Characterization of Single-Crystal Films

The occurrence of heteroepitaxy, which was suggested by the surface morphology of the as-grown films, was substantiated by x-ray diffraction. Back-reflection Laue patterns were obtained from three widely separated locations on a CdTe film 2.5 cm across and  $17.8 \mu\text{m}$  thick on muscovite mica (specimen M81), viz., from the center and from the periphery at either end of a diameter. In addition, the pattern from the mica substrate was recorded from the opposite face of the specimen, in order to permit the unequivocal identification of mica contributions to the film pattern. The three CdTe patterns were identical, indicating the absence of mutual misorientation within the sensitivity of the technique. It was concluded that the region spanned by the sampled areas is a single crystal. Additional patterns from this and other CdTe/mica specimens confirmed the single-crystal nature of the films.

The macroscopic appearance of the films suggests that each is comprised of several large subgrains, perhaps induced by substrate flexure during deposition. (See Figure 11c in Section 2.3.3 for a typical example.) Back-reflection Laue patterns with the x-ray beam straddling apparent subgrain boundaries failed to reveal fragmentation in all but one case, where a double pattern with a mutual misorientation less than or equal to  $2^\circ$  was observed.

A typical back-reflection Laue pattern from the CdTe film of specimen M81 is presented as Figure 5(a). It shows a high degree of symmetry and is readily interpreted to reveal the following orientation relationship:



i.e., the close-packed double layer of CdTe, which is polar and has trigonal symmetry, is parallel to the unique  $(\text{Si}_3\text{Al})\text{O}_{10}$  hexagonal net of the mica. This is the heteroepitaxial relationship predicted on general grounds and observed previously.<sup>(3)</sup> The patterns were indexed according to cubic-system symmetry, since Debye-Scherrer analysis of as-deposited films had shown them to have the sphalerite structure of the cubic polymorph rather than the wurtzite structure of the hexagonal polymorph.

Nevertheless, the CdTe patterns exhibit excess symmetry for a cubic crystal, being six-fold rather than three-fold. This is interpreted as evidence that the films are heavily twinned, a result which is to be expected because of the high degree of pseudosymmetry inherent in the sphalerite structure. As shown in Figure 5, the patterns are consistent with the sphalerite twinning operation:  $180^\circ$  rotation about the normal to (111).

The results of the back-reflection Laue analysis were further corroborated by the diffractometer method used in the reflection geometry. The following observations were made:

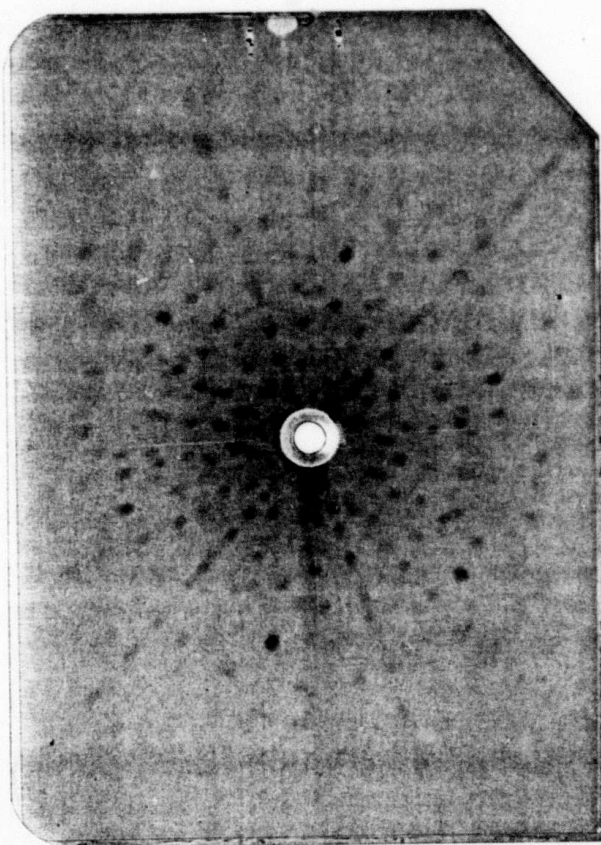
- The diffraction patterns from various regions of the same CdTe/mica specimen match, indicating that the film is a single crystal.
- The diffraction peaks comprising the patterns have the relative intensities and angular positions to be expected for a CdTe single crystal of cubic symmetry.
- Rotation of the specimen in its own plane causes all diffraction peaks except 111 to pass through intensity minima (detuning), indicating that the film is a single crystal with (111) parallel to the substrate surface.

#### 2.2.5 Films Deposited on Other Substrates

In the initial series of experiments, when the results on mica were poor, different substrate materials were tried to determine the effects of varying thermal properties and crystal structure. The substrate materials were sapphire and silicon.

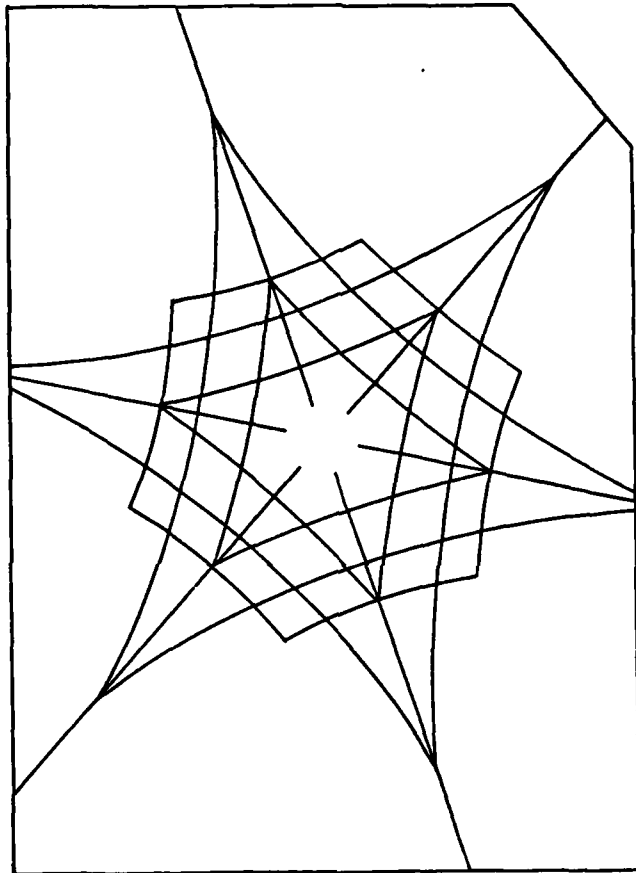
Two different crystal orientations of sapphire were used, with the c-axis either normal or parallel to the surface. Four different silicon substrates were used, all with (100) orientation. They were (1) polished, (2) polished with a thermally grown oxide layer of 0.1 micron, (3) etched to give polyhedral etch pits bounded by (111) faces about 1 micron deep, and (4) same as in (3) but with a thermally grown oxide less than 0.1 micron thick. The texture-etched silicon substrates were used by Spire for graphoepitaxy experiments (see Section 2.3.4).

The deposited films in all of these cases were fine-grained polycrystalline CdTe. This provided strong evidence for modification of the deposition apparatus being necessary for epitaxial film growth. Experiments with these substrates were not yet complete, after the modifications were made, at the time of this report.



(a)

FIGURE 5. Back-reflection Laue pattern from CdTe film on muscovite mica (specimen M81). (a) Pattern as recorded, negative image; molybdenum radiation, 20 kV/20 mA, 5 h exposure. (b) Important zone hyperbolae of the pattern, showing the 6-fold pseudosymmetry of the twinned crystal. (c) and (d) Components of the pattern, showing the 3-fold symmetry of the untwinned crystal in (111) orientation, with the prominent diffraction maxima indexed; the two components are related by the twinning operation:  $180^\circ$  rotation about the normal to (111).



(b)

R40362

FIGURE 5. (Continued)

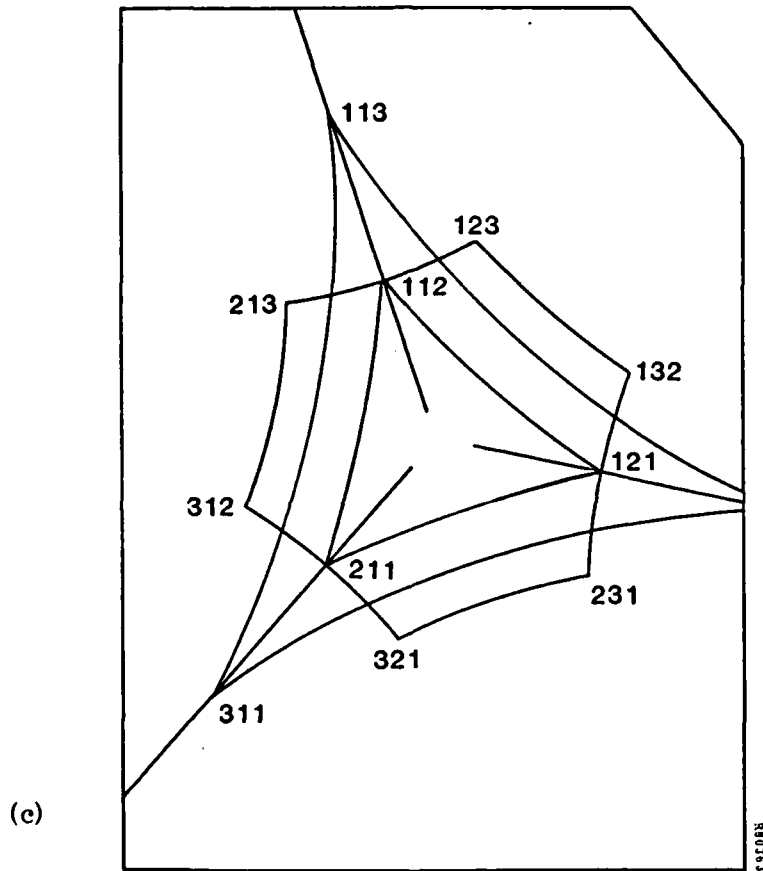


FIGURE 5 (Continued)

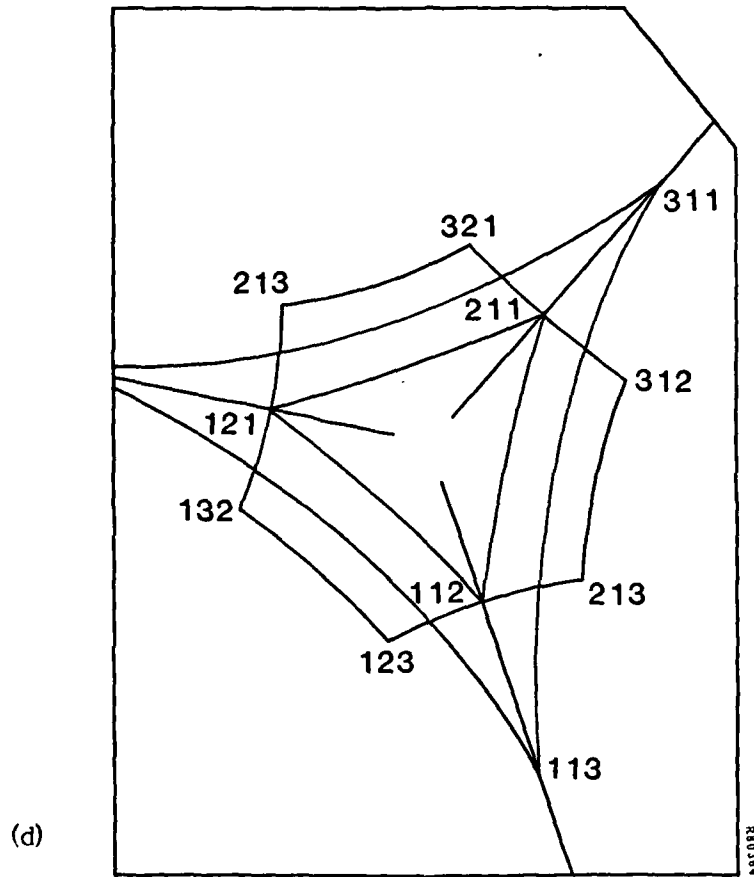


FIGURE 5. (Concluded)

## 2.3 PULSED ELECTRON BEAM PROCESSING OF CdTe FILMS (TASK 2)

### 2.3.1 Objective

The objective of this task is to produce single-crystal CdTe films with minimal defects.

There are two distinct approaches. The films deposited by evaporation directly upon crystalline substrates are expected to be epitaxial, but with defects such as microtwins. Directed energy processing, with very fast crystal growth rates, is expected to reduce the density of such defects, as observed for silicon.<sup>(9)</sup> The second approach, termed graphoepitaxy, will be tested to determine if pulse processing can produce single-crystal crystal films on patterned, amorphous substrates.

### 2.3.2 Equipment

The pulsed electron beam equipment used in this experiment has been described before.<sup>(10)</sup> Briefly, it consists of a d.c. charged transmission line, which is rapidly switched into a diode load. The pulse width is fixed by the electrical characteristics of the discharge circuit. The electron energy is varied by changing the impedance of the field emission diode, and the current density is changed by altering the focusing of the beam. The electron beam diameter can be changed from 0.5 to 10 cm. For these experiments, the electron energy spectrum is given in Figure 6, and the resulting energy deposition profile in CdTe in Figure 7. The heating of the sample is controlled by altering the total energy per unit area delivered (the fluence). This figure (fluence), quoted in joules/cm<sup>2</sup>, is included in the description of each experiment.

A recent addition to this apparatus is the heated sample stage shown in Figure 8. Temperatures from 20 to 400°C can be achieved and monitored. There is no appreciable change in average sample temperature as a result of the pulse process, which heats only a few microns of material. This apparatus will be used to test the effect of annealing of Hg ion implanted into CdTe (Task 4).

In the opposite direction, samples may be cooled during pulsing down to 77°K (or lower by special arrangement) using the cryostat shown in Figure 9. This apparatus was used for experiments (in Task 4) where Hg was evaporated onto a cooled CdTe sample and then pulse heated. When the sample was warmed up to room temperature, Hg was found to be stably bound to the surface.

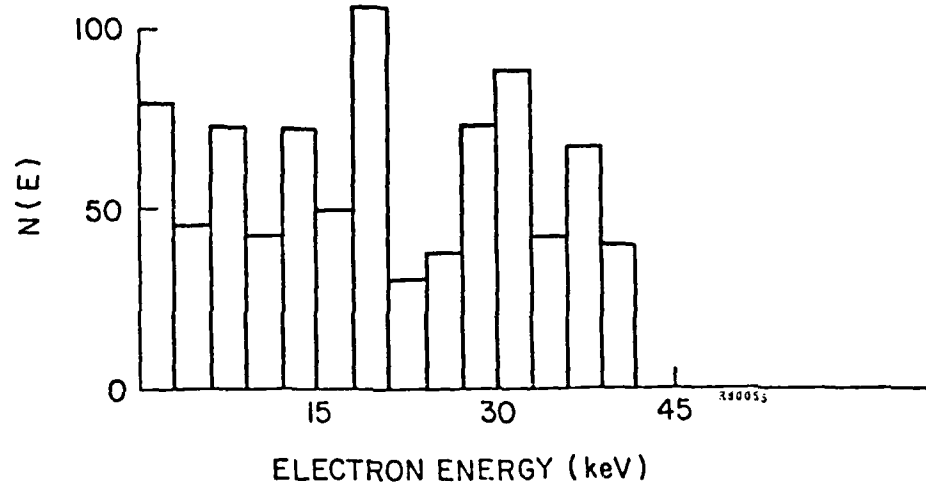


FIGURE 6. Electron energy spectrum of beam used to process CdTe

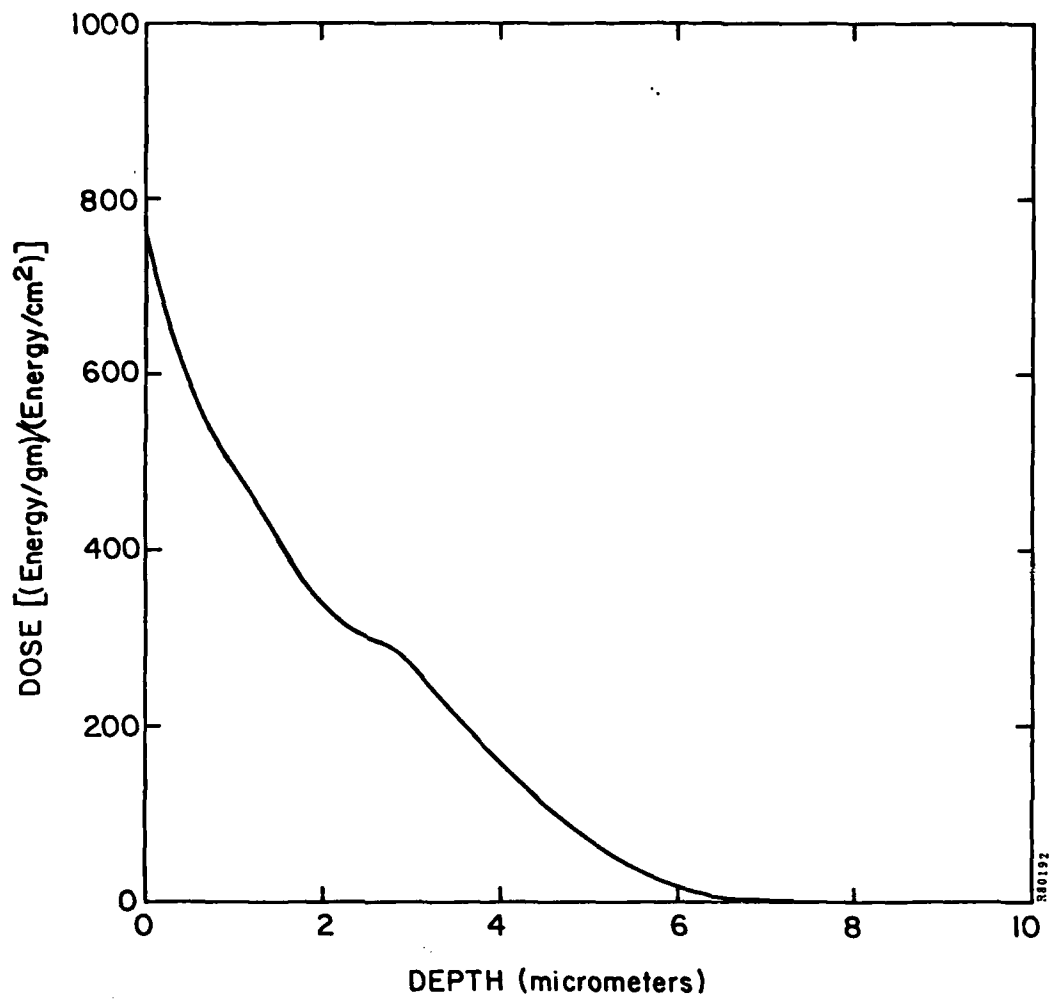
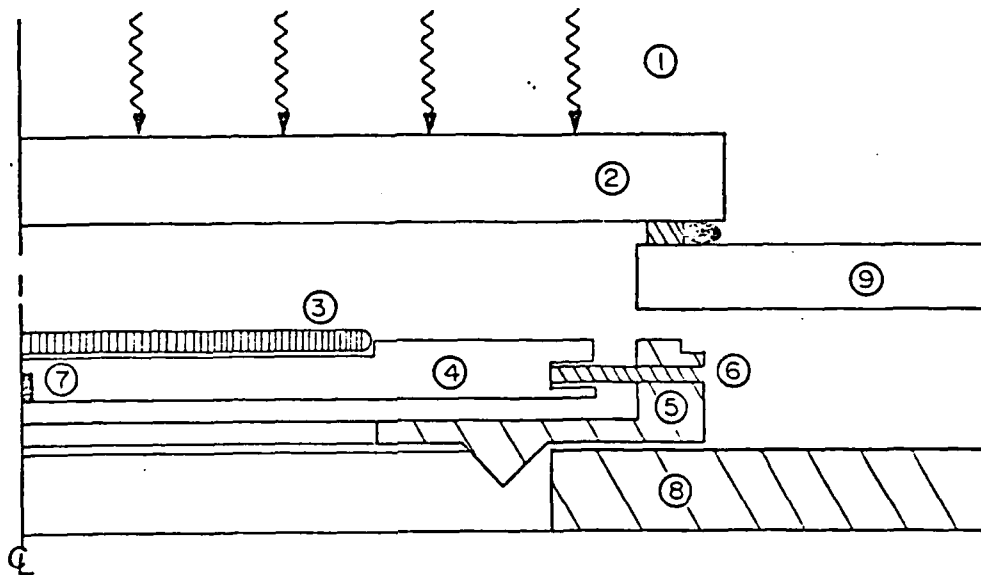


FIGURE 7. Deposition profile of electron beam in CdTe using the energy spectrum of figure 6 at a 45° angle of incidence



1. Radiant heat source, outside of vacuum chamber.
2. Glass port, air cooled.
3. Two-inch sample with CdTe film.
4. Carbon disk.
5. Aluminum disk (normal holder assembly).
6. Set-screw thermal isolation (8).
7. Thermocouple (wires not shown).
8. Carousel for transport to diode.
9. Vacuum chamber top.

FIGURE 8. Heated sample stage for pulsed electron beam apparatus

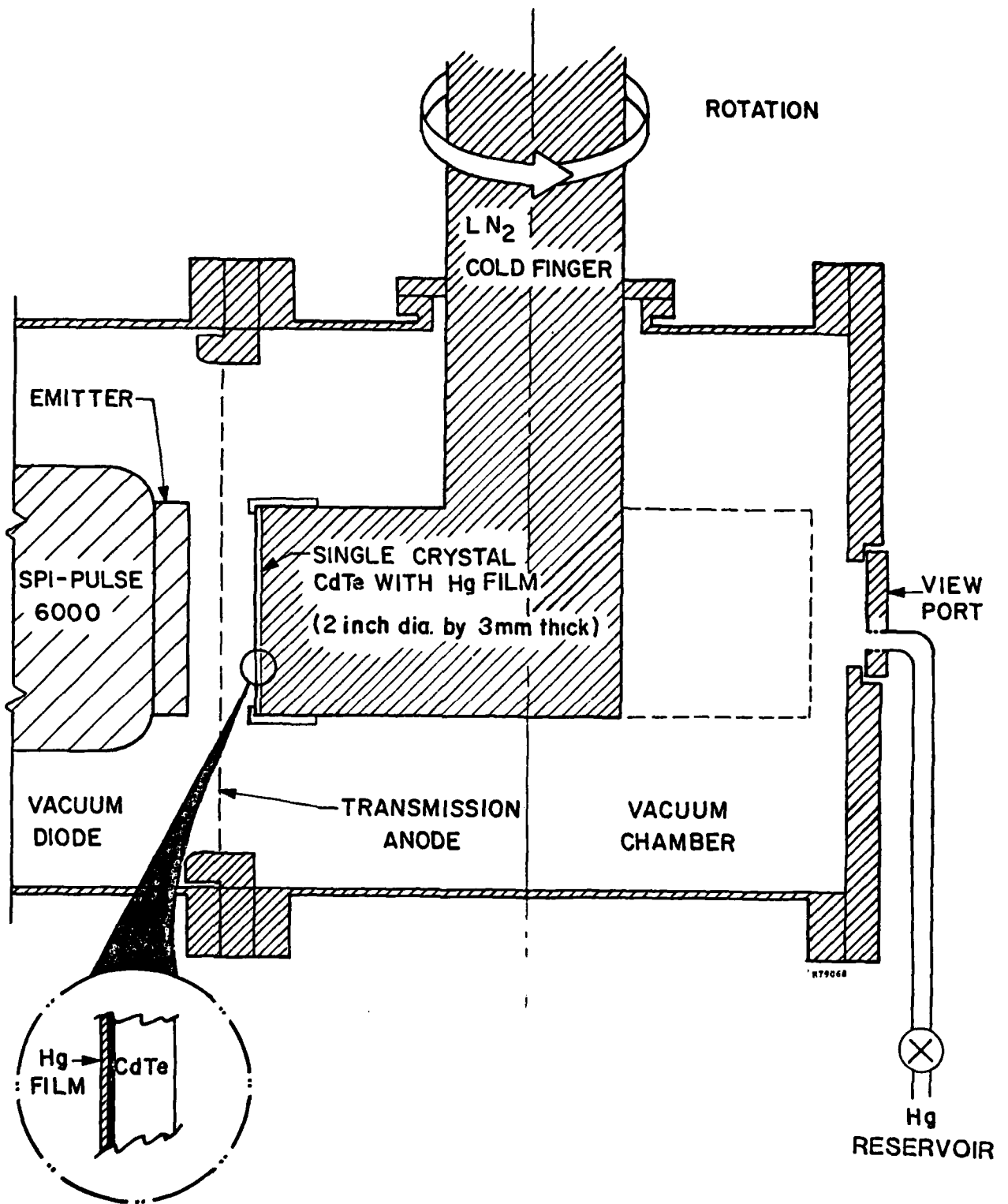


FIGURE 9. Cryogenic cooled sample stage for pulsed electron beam apparatus

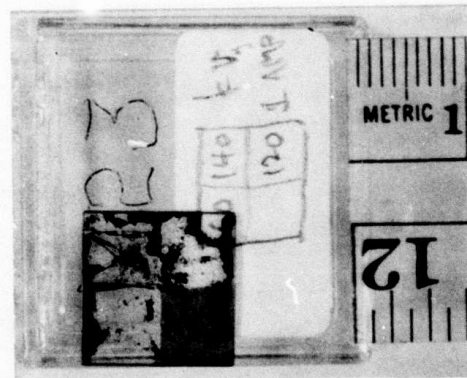
### 2.3.3 Heteroepitaxy Results

As previously reported,<sup>(1)</sup> pulse processing was defined for bulk CdTe. Initial experiments in this reporting period sought to define the process for thin films on insulating substrates. Suitable films deposited on mica by NERC were furnished to Spire for the pulse treatment. Typical results are pictured in Figure 10.

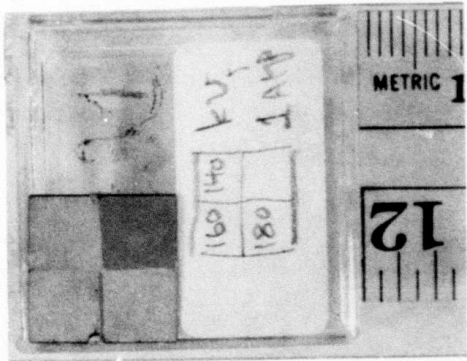
The CdTe films shown in Figure 10 were respectively (a) 0.4  $\mu\text{m}$ , (b) 11  $\mu\text{m}$ , and (c) 2.3  $\mu\text{m}$  thick. The films in (a) and (b) were deposited before the modification to the hot wall apparatus discussed in Section 2.2.2; the film shown in (c) was deposited after the modification. To take maximum advantage of a limited number of samples, the pulse region was restricted to an area 0.5 by 0.5  $\text{cm}^2$  using a 0.5 mm thick carbon mask. Some interaction between the beam and the mask caused the fluence near the corners to be enhanced (visible in Figure 11(b)). Three different fluences were used to irradiate samples (a) and (b), but only one pulse was used on sample (c). Data are given in Table 1.

The adherence of these films to the (mica) substrate was poor. A tape test removed part of sample (c) in Figure 10 (upper right-hand corner). This is possibly the result of mismatched thermal expansion parameters between mica and CdTe. Possibly better results will be achieved on sapphire or quartz. The poor adhesion, combined with electrostatic forces, led to the blowoff of the thinnest film (0.4 micron) pulsed on mica. The sheet resistance of the film was insufficient to carry the beam current (500  $\text{A}/\text{cm}^2$ ) without a large potential drop. Hence the film blew off. This did not occur for films of practical interest, over 2 micron, as shown in (b) and (c). This blowoff problem did not occur for similar test films on sapphire or oxidized silicon wafers. Pulsed electron beams can be used to process CdTe films on insulating substrates.

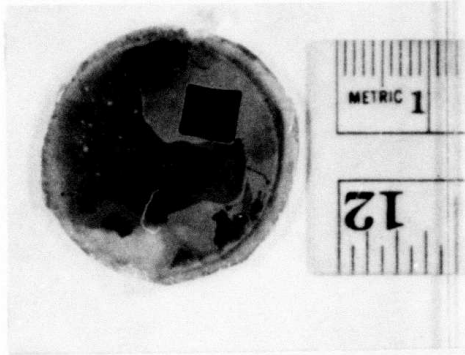
The structure of these films was examined by SEM, with EDAX, and by x-ray diffraction. Those samples (Figures 10 a and b) deposited before the modification of the evaporation apparatus were polycrystalline before and after pulsing. There was no discernable change in the bulk stoichiometry. Sample (c) has not yet been characterized completely. Pulsing at a fluence high enough to insure melting the entire depth of film improved the surface quality; it became smoother and more reflective. Thus, the area pulsed (Figure 10c) appears black because of specular reflection from the oblique illumination.



(a) 0.4  $\mu\text{m}$



(b) 11  $\mu\text{m}$



(c) 2.3  $\mu\text{m}$   
(Epitaxial film)

FIGURE 10. CdTe films on mica pulsed electron beam treated in 5mm x 5mm regions.

TABLE 1. PULSED ELECTRON BEAM PROCESSING PARAMETERS  
FOR SAMPLES SHOWN IN FIGURE 10

Sample	Reference Voltage (V)	Fluence (J/cm <sup>2</sup> )
(a)	120	0.20
	140	0.31
	160	0.46
(b)	140	0.31
	160	0.46
	180	0.65
(c)	180	0.65

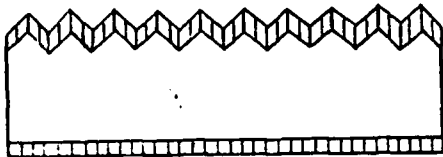
#### 2.3.4 Graphoepitaxy Results

The graphoepitaxy process investigated by this research program is depicted in Figure 11. A (100) silicon wafer is etched anisotropically to produce a pyramid pattern with (111) faces atomically smooth and joined at exceedingly sharp corners (Figure 12a). This surface may be covered by a thin (~10 nm) oxide or replicated in a material to be specified later. The replication may be a positive or a reverse image. The pattern is now covered by an amorphous CdTe film (Figure 12b), sufficiently thick to fill all valleys with a smooth surface when melted. The film is pulse melted in a way that does not melt the patterned substrate. Upon rapid cooling, the film is oriented by the pattern, which corresponds exactly to a cubic structure. It is believed that the film will cool with one preferred crystal orientation induced by the patterned substrate. Furthermore, since the pattern was based on a perfect single crystal, all points in the film (which may cool at slightly different times or rates) should be in registry, and the film will become a single crystal!

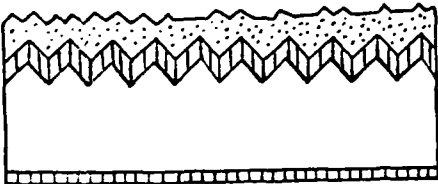
The possibility of crystal alignment of a thin film to a pattern etched into an amorphous substrate was demonstrated by H. Smith<sup>(11)</sup>. This is a variant on that process, pursued as an alternative when the initial evaporated CdTe films were not epitaxial on the crystalline substrate. In these experiments, CdTe films were deposited directly on etched silicon, or oxidized etched silicon, only. The initial results were no different from films deposited on unetched surfaces. However, the results may not be taken as conclusive, because the deposited films had poor composition due to the faulty, initial hot wall reactor. The experiment will be repeated with better samples as a check. Note, in Figure 12c, that the surface after pulsing is smooth due to melting.



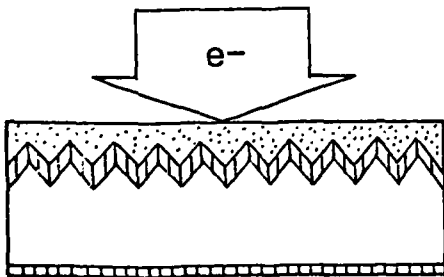
- Texture etch (100) silicon ( $\sim 1 \mu\text{m}$  features)



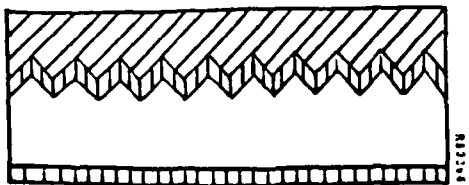
- Grow thin ( $\sim 100\text{\AA}$ ) thermal oxide



- Deposit CdTe ( $\geq 3 \mu\text{m}$ )

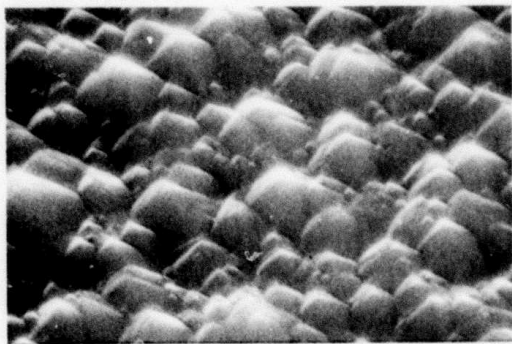


- Pulse with electron beam
- Recrystallize to single crystal film



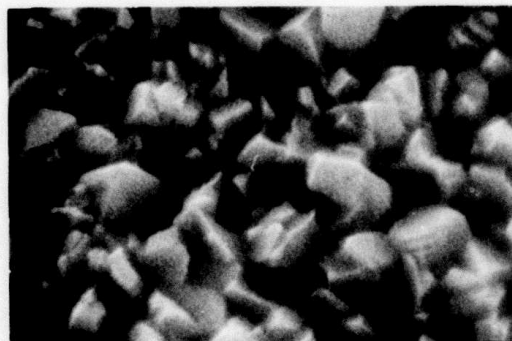
- Isothermal growth of HgTe and diffusion

FIGURE 11. Schematic of graphoepitaxy process



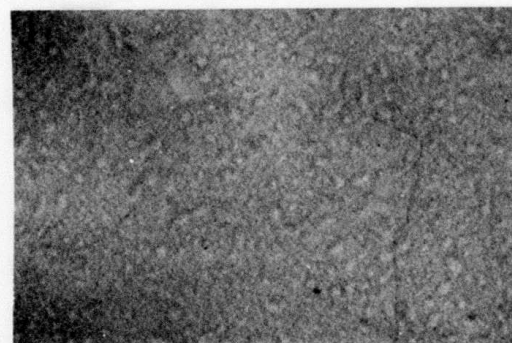
1  $\mu\text{m}$

(a) Etched silicon substrate



1  $\mu\text{m}$

(b) Above with 2.5  $\mu\text{m}$  CdTe film (as deposited)



1  $\mu\text{m}$

(c) Above after pulsed electron beam heating at 0.65  $\text{J}/\text{cm}^2$

FIGURE 12. Graphoepitaxy experiment.

The results to date are shown in Figure 12. At the top is a picture of the texture etched silicon surface with typical 1 micron pyramids. This structure was covered with CdTe (center) and pulsed (bottom). As deposited, the film surface resembled the surface of any other CdTe film deposited in the hot wall reactor prior to modification. There was no discernable change in texture between Figure 12b and the unpulsed, magnified surface of Figure 10b, for example. Note that the film thickness was more than twice the height of the pyramids. After pulsing at a fluence ( $0.65 \text{ J/cm}^2$ ) which would melt the entire film, the surface was generally smooth (Figure 12c) and had greatly increased specular reflectivity. However, the film was polycrystalline as determined by RHEED (reflected high energy electron diffraction) analysis.

## 2.4 VAPOR EXCHANGE OF CdTe TO FORM HgCdTe (TASK 4)

### 2.4.1 Objective

The objective of this task, performed at NERC, is to convert thin-film CdTe to  $\text{Hg}_{0.8}\text{Cd}_{0.2}\text{Te}$  by vapor exchange. The task comprises the construction of a suitable apparatus, the establishment of isothermal growth conditions, and the characterization of the resultant films.

### 2.4.2 Process Considerations

The process of isothermal growth of HgCdTe solid solution films consists of three steps:

- sublimation of HgTe
- deposition of the vapor components (Hg and  $\text{Te}_2$ ) onto the surface of the CdTe film
- diffusion of the deposited components into the layer

In these experiments, performed at NERC, the isothermal growth process was carried out in a sealed quartz ampoule illustrated in Figure 13. The ampoule was loaded with the CdTe film (c) on a suitable substrate (T), a HgTe source (H), and some pure mercury. The following considerations were used to determine the relative amounts for each material.

The concentration of the metallic components of the solid solution depends upon the mass ratio of HgTe to CdTe. For the composition  $\text{Hg}_{0.8}\text{Cd}_{0.2}\text{Te}$ , this mass condition is:

$$M_H/M_C = 5.47$$

where  $M_H$  is the mass of the HgTe charge and  $M_C$  is the mass of the CdTe film. A small correction to this condition is the excess of volatile components (over the desired composition) which are present in the vapor phase in the ampoule during isothermal

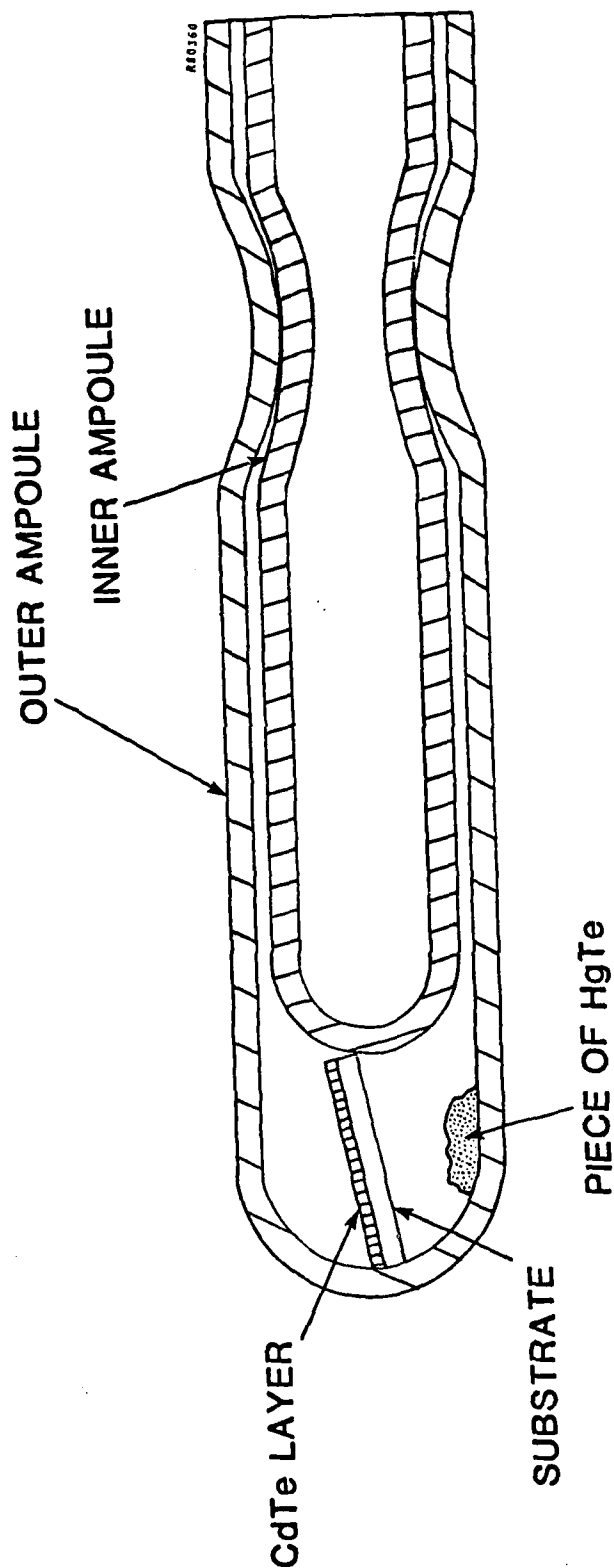


FIGURE 13. Schematic of vapor exchange apparatus (at NERC)

growth. The components which remain in the vapor phase do not contribute to the diffusion process. To avoid a change in composition, an excess amount of the volatile components must be added to the ampoule. This excess amount depends upon the sealed volume of the ampoule, the process temperature, and the partial vapor pressure of the volatile components.

The dominant component of the vapor phase inside the sealed ampoule is mercury. This implies that a definite but small amount of Hg must be added to the ampoule which is equal to the mass of vapor at the growth temperature. This in turn requires a measurement of the inner volume of the ampoule before it is sealed. Note that the vapor pressure of Hg given in the literature<sup>(12,13)</sup> has an exponential dependence upon the temperature. Therefore, during isothermal growth only a small correction of the temperature is needed to reach equilibrium conditions inside the ampoule.

A hydrostatic method was used to determine the inner volume ( $V_i$ ) of the ampoule. The formula is:

$$V_i = \frac{M_1(1/d_L - 1/d_Q) + M_T(1/d_Q - 1/d_T) + M_H(1/d_Q - 1/d_H) + M_C(1/d_T - 1/d_C) - M_2/d_L}{1/d_Q}$$

where  $M_1$  and  $M_2$  are the mass of the sealed ampoule in the air and in the measuring liquid, respectively;  $d$  is the density of the specified component; and subscripts L, Q, T, H, and C designate liquid, quartz, substrate, HgTe, and CdTe, respectively. This technique was sufficiently accurate to yield good results.

#### 2.4.3 Initial Results

Three HgCdTe layers were grown by this technique using polycrystalline CdTe films obtained from the original furnace design. The resulting  $Hg_{1-x}Cd_xTe$  films were also polycrystalline with inhomogeneous value of  $x$ . Apparently, a better quality epitaxial layer of CdTe is necessary for isothermal growth of HgCdTe. The growth temperature for these experiments was 550°C; and the time the sample was held at this temperature for deposition and diffusion was 168 hours (7 days).

An additional sample was completed just prior to writing this report. The initial CdTe film was from the modified hot wall reactor and was epitaxial prior to vapor exchange. The finished HgCdTe film has an excellent quality surface, and preliminary indications are that it is a single crystal.

#### 2.4.4 Film Characterization

NERC used an external vendor to check the composition of the HgCdTe (vapor exchange) films using EDAX. The results of this analysis are given in Table 2, where they are compared to the EDAX analysis of a "standard"  $\text{Hg}_{0.8}\text{Cd}_{0.2}\text{Te}$  sample. The discrepancies in true composition are due to faulty analysis. Initial results when Spire used a different vendor for EDAX analysis of CdTe showed a marked dependence upon the energy of the electron beam used (Table 2). Since the raw signal data is extensively analyzed by a computer, it must be concluded that the typical computer codes do not accurately characterize materials at low electron energies. The qualitative interpretation of the data in Table 2 is that the composition near the center of the sample was close to that desired, whereas the composition at the edge of the sample was significantly in error.

Other methods used for film characterization include Laue x-ray diffraction patterns and the Debye method, IR transmission, and electrical resistance measurements. The Debye-Scherrer method was used to determine the spacing of the unit cell of the CdTe films. A typical infrared spectrum for HgCdTe films (polycrystalline samples) is shown in Figure 14. There is a very gradual absorption edge. This is attributed to the initial nonepitaxial CdTe film used to fabricate this sample.

An x-ray diffraction setup was recently installed at NERC. This will increase the quantity of data, since all x-ray measurements to date had to be performed by outside vendors. About half of this outside work was performed for Spire, half for NERC.

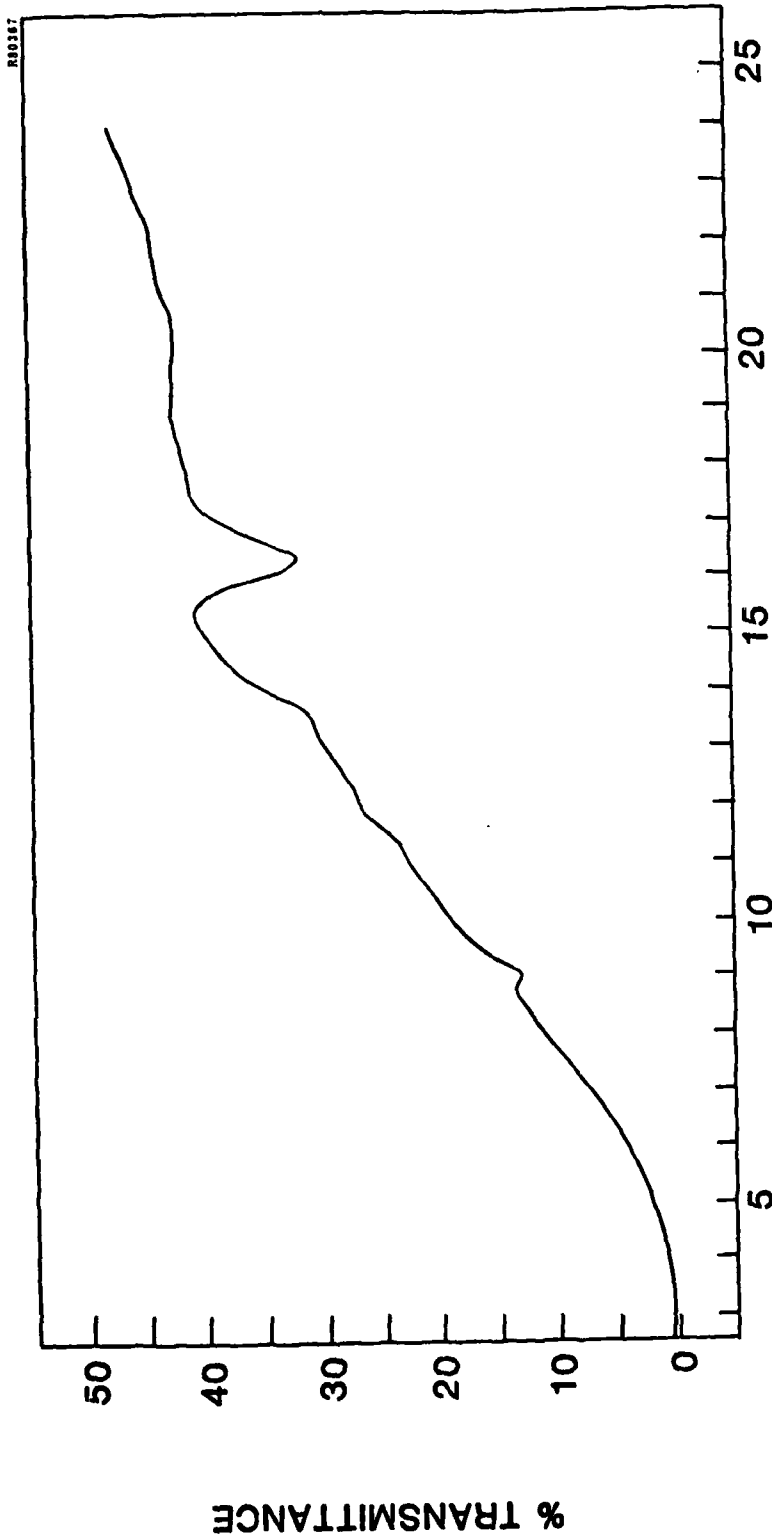
### 2.5 MODIFICATION OF CdTe BY ION IMPLANTATION (TASK 4)

#### 2.5.1 Objective

The goal of this task is to modify the composition of thin single-crystal CdTe films (Task 2) to HgCdTe with the appropriate composition. The approach is to implant Hg and Te and then pulse or thermally anneal the film.

#### 2.5.2 Implantation and Pulse Annealing Results

Mercury was implanted in bulk CdTe at 50 keV and at 5 keV. High total doses were used to assess the composition and film thickness which would be reached. Part of each implanted sample was pulse annealed, and pre- and post-pulse results compared. Summarizing the results, the sputtering coefficient of Hg ions at 5-50 keV incident upon CdTe was so great that neither high Hg concentrations nor thick films of HgCdTe could be achieved. An alternate technique, evaporation of Hg onto a cooled substrate, to be followed by implantation of Te and then pulse annealing, is reported in the next section.



WAVELENGTH (microns)

FIGURE 14. Infrared transmission spectrum of CdTe film enriched in Hg by vapor exchange (specimen Si 39)

TABLE 2. EDAX ANALYSIS OF CdTe AND HgCdTe

a) NERC Analysis of Sample Number 43

Component	Measured at.-% (at center)	Measured at.-% (at edge)
Te	38.32	84.24
Cd	4.36	11.46
Hg	57.32	4.31

b) NERC Analysis of Known Bulk  $\text{Hg}_{0.8}\text{Cd}_{0.2}\text{Te}$  Sample

Component	Measured at.-%
Te	40.59
Cd	8.76
Hg	50.64

c) SPIRE Analysis of Known Bulk CdTe

Component	Measured at.-% at 5 keV	Measured at.-% at 15 keV
Te	$67.86 \pm 1.8$	$50.81 \pm 1.2$
Cd	$32.14 \pm 6.8$	$49.19 \pm 1.7$

The high current ion implanter at Spire Corporation was modified for these implants with the addition of an oven for solid sources and a sample holder for thick (3 mm) wafers. Purified  $\text{HgCl}_2$  was used as a source of mercury. The implanter was initially set to admit isotopes  $^{200}\text{Hg}$  through  $^{202}\text{Hg}$ , to maximize the beam current (approximately 200 microamperes at 50 keV). This ion beam is scanned for 100 mm wafers, so the current density on the samples was  $2 \text{ A/cm}^2$ . At 50 keV this was a power input of  $0.1 \text{ W/cm}^2$ , and the sample could have been heated.

The sample holder was rotated during implantation and was therefore not actively cooled. As a worst case estimate of sample temperature (which was not monitored during implantation), radiation cooling from two sides can be assumed with an (approximate) emissivity of 0.5. At  $0.1 \text{ W/cm}^2$  input this implies a sample temperature of  $91^\circ\text{C}$  at equilibrium. This value was considered acceptable. At 5 keV there would be a negligible temperature rise.

The implant time was 2 hours for a dose of  $10^{17}$  ions/cm<sup>2</sup>. This long period would allow contamination buildup as a result of residual vacuum chamber deposits on the sample being "knock-on" implanted; i.e., a Hg ion impinges upon an atom (C, H, or O) on the sample surface and "knocks" it into the CdTe. This effect was minimized through the use of a cryopump installed on the end station of the implanter. Measurements were not made on this program for such efforts, but other work<sup>(14)</sup> indicates that the cryopump did reduce hydrocarbon contaminants below detectable levels, whereas diffusion pumped systems degraded device performance when the implant took a long time.

Ion implanted samples were pulse annealed in the apparatus described in Section 2.3.2. The total fluence was held fixed at  $0.9 \text{ J/cm}^2$ . Samples implanted at 50 keV to a dose of  $10^{15}$ ,  $10^{16}$ , or  $10^{17}$  ions/cm<sup>2</sup>, and at 5 keV to  $10^{16}$  ions/cm<sup>2</sup>, were pulse annealed. Analysis compared as-implanted with post-pulse annealed samples. A comparison to thermal annealing was not attempted in view of these results.

Samples were analyzed in the order of increasing complexity and cost by EDAX, Auger spectroscopy, and IMMA. X-ray analysis of composition on an SEM was used as a survey technique. Mercury was not detected in any CdTe samples which were implanted at an energy of 50 keV, even at the maximum dose of  $10^{17}$  ions/cm<sup>2</sup>. At 5 keV and a dose of  $10^{16} \text{ Hg}^+/\text{cm}^2$ , a trace amount (about 1 percent) of mercury was detected by EDAX in the CdTe samples before pulse annealing. After annealing this element could not be detected. Presumably the surface concentration was reduced below the detection limits by diffusion during the anneal process.

Hg Area (10.17 keV) vs SPUTTERING TIME

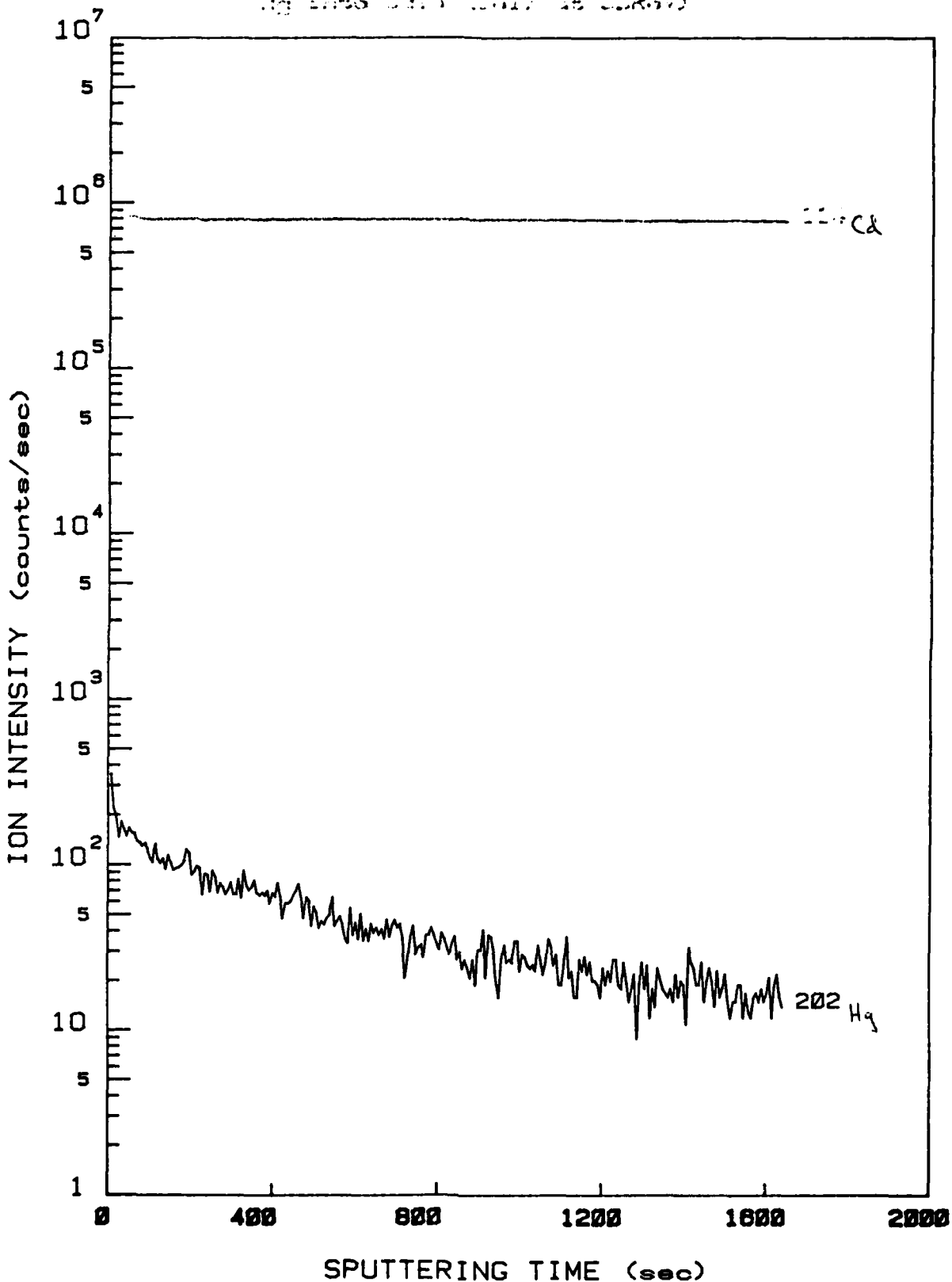


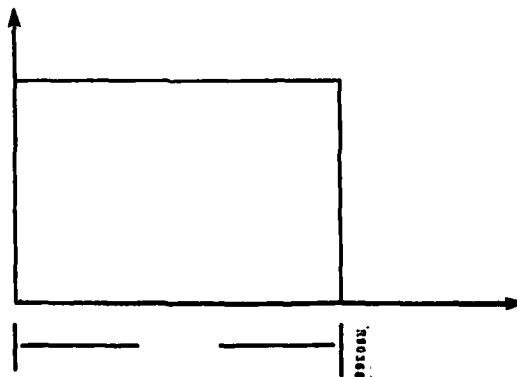
FIGURE 15. IMMA depth profiles of Cd and Hg in ion implanted CdTe  
2-30

Auger spectroscopy was used to analyze the high dose 50 keV implanted samples, the 5 keV implants, and the cryo-evaporation (Section 2.5.4). After this work it was reported<sup>(15)</sup> that Auger spectroscopy was a poor technique for analysis of HgCdTe because the analyzing electron beam dissociates the material, preferentially removing the mercury from the surface. This effect could be seen when analyzing a "standard"  $\text{Hg}_{0.8}\text{Cd}_{0.2}\text{Te}$  sample with Ar ion sputtering for a depth profile. The signal for Hg did not stabilize for the first 3 minutes (approximately 3000A) of sputtering. However, as the analysis failed to detect any Hg in any implanted sample, the accuracy of the technique did not affect the results. The minimum detectable Hg concentration, as determined by the "standard" sample, was about 1 atomic percent. Since we were looking for a concentration level of 40 atomic percent Hg, and found none, experiments with ion implantation were stopped.

One sample, CdTe with a 50 keV implant of  $10^{17} \text{Hg}^+/\text{cm}^2$ , was submitted for IMMA (ion microprobe mass analysis). This is similar to SIMS, but with greater sensitivity and better depth profiling by raster scanning the sputtering ion beam. The result is shown in Figure 15. A rough concentration scale can be placed on the counts/sec with the (admittedly poor) assumption that the sensitivity of the detector signal to Hg and Cd is identical. The flat Cd signal is proportional to the 50 percent (atomic) constituent; the isotope  $^{114}\text{Cd}$  is 28.86 percent of the total Cd. The isotope of mercury,  $^{202}\text{Hg}$ , detected (mass 200 was not detected) would be 69 percent of all Hg in the sample of both isotopes 201 and 202 were implanted. The peak (surface) concentration of Hg shown in Figure 15 is then 100 ppm. This low value plus the shape of the curve imply that the implanted concentration is dominated by ion sputtering effects which are analyzed in the next section.

### 2.5.3 Analysis of High-Dose Implantation of Hg into CdTe

Consider the implantation of Hg into CdTe, using the treatment of Liau and Mayer<sup>(16)</sup>.



The flux of incident Hg ions  $J_i$  produces a uniform atomic mixture containing an implanted Hg concentration  $N_{\text{Hg}}$  and extending to a depth  $W$  below the surface; it also induces back-sputtered fluxes of both the implanted species  $J_{\text{Hg}}$  and the target species  $J_B = J_{\text{Cd}} + J_{\text{Te}}$ .

The steady-state or maximum achievable concentration of Hg is:

$$N_{\text{Hg}}/N_B = r/(S-1)$$

where the concentration of target species  $N_B$  comprises Cd and Te.

$r$  is the preferential sputtering probability of the target species relative to Hg.

$$r = (J_B/J_{\text{Hg}})$$

$S$  is the total sputtering yield

$$S = (J_{\text{Hg}} + J_B)/J_i$$

#### Preferential Sputtering Probabilities

According to Anderson,<sup>(17)</sup> mass difference effects dominate sputtering from the target at all implant energies significantly above the threshold, with the light component preferentially sputtered; this becomes more pronounced as the mass of the projectile ion increases.

The preferential sputtering of the light component was confirmed by Liao et al.<sup>(18)</sup> for the 20-80 keV energy range and by Lewis and Ho<sup>(19)</sup> for the low keV range. Their results suggest the following:

- For target species of different masses, the relative sputter yield is approximated by the inverse mass ratio.
- For target species of closely similar masses the relative sputter yield is approximated by the ratio of the sputter yields of the pure (atomic) components.
- The steady-state surface composition is independent of the energy of the projectile ions, whereas the thickness of the altered layer increases with increasing ion range.

Evaluation of Preferential Sputtering Probabilities of Cd and Te Relative to Hg

$$N_{\text{Hg}}/N_{\text{B}} = r/(s-1)$$

$$r = J_{\text{B}}/J_{\text{Hg}}$$

$J_{\text{Cd}}/J_{\text{Hg}}$	mass Hg/mass Cd
	200.59/112.40
	1.8

$J_{\text{Te}}/J_{\text{Hg}}$	mass Hg/mass Te
	200.59/127.60
	1.6

$r$	$(J_{\text{Cd}} + J_{\text{Te}})/2J_{\text{Hg}}$	1.7
$N_{\text{Hg}}/N_{\text{B}}$	$1.7/(S-1)$	

This steady-state concentration obtains after the sputter-removal of a thickness  $rW$ , where  $W$  can be identified with the range of the ions. This last equation is plotted in Figure 16. From it and Figure 15, the implied sputtering coefficient of 50 keV  $\text{Hg}^+$  incident upon CdTe is over 1000.

#### 2.5.4 Evaporation and Pulse Diffusion Results

Evaporation and pulse diffusion of thin layers have been shown to produce epitaxial crystalline layers in semiconductor materials<sup>(20)</sup>. Because sputtering effects seemed to rule out ion implantation of Hg as a means of forming HgCdTe layers a few microns thick from CdTe, evaporation and pulse diffusion were tried as an alternate approach. Using the apparatus shown in Figure 9, two experiments were performed. Mercury vapor from a heated ( $\sim 100^\circ\text{C}$ ) source was directed against a crystalline, bulk CdTe sample held at  $77^\circ\text{K}$  (liquid nitrogen cooled). When a visible layer accumulated, the sample was turned around and pulse heated by an electron beam (in vacuum). This experiment was repeated using a different portion of the same substrate, iterating the evaporation-pulse procedure four times. The sample was then heated to room temperature and analyzed.

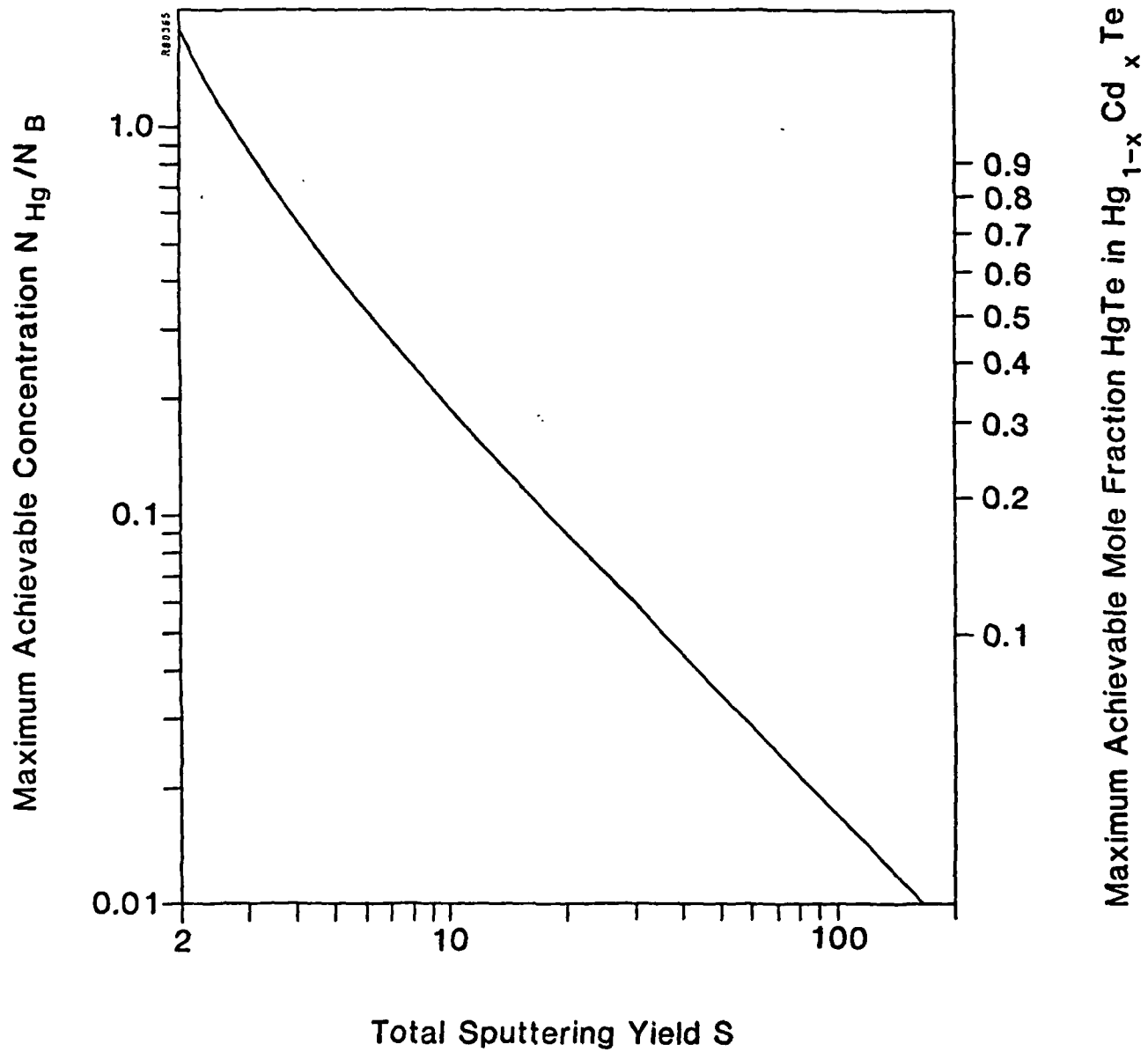


FIGURE 16. Concentration  $x$  of  $\text{Hg}_{1-x}\text{Cd}_x\text{Te}$  as a function of sputtering yield for  $\text{Hg}^+$  implanted into  $\text{CdTe}$

The two pulsed areas had a distinct silvery appearance which did not change when warmed up to 25°C or taken out of the vacuum chamber. Analysis by an SEM showed the surface of the singly pulsed sample had a fine scale ( $\leq 1 \mu\text{m}$ ) texture. In the RBEI (Robinson Backscattering Electron Imaging) mode the composition of this surface appeared nearly uniform. Auger analysis indicated that the Hg content in a region within 0.1 micron of the surface was between 1 percent and 10 percent. The sample which had been pulsed 4 times had a rough surface but also had a Hg content over 40 (atomic) percent. Level of effort permitting, the experiment will be repeated with combined Hg evaporation and Te implantation (or vice versa) to achieve the correct composition.

## SECTION 3 FUTURE PLANS

### 3.1 DEPOSITION AND PULSED EPITAXY

Since the quality of the deposited films has improved with the modification to the hot wall furnace, many of the initial experiments will be repeated. These tests include evaporation onto quartz, two orientations of sapphire, and etched silicon. These films will be pulsed and examined for crystallinity and composition. A comparison of pulse and non-pulse processed films after HgTe vapor exchange will be made. Graphoepitaxy experiments will be de-emphasized since the heteroepitaxy results have improved so dramatically.

### 3.2 EVAPORATION AND CASCADE IMPLANTATION

Mercury implantation has produced extreme ion sputtering effects. Co-implantation of Hg and Te to change thin CdTe films to HgCdTe is therefore not directly possible. Cascade implantation will be tested. The evaporation of a thin layer of Hg (or Te) followed by ion implantation of Te (or Hg), or alternately the co-evaporation of both Hg and Te followed by ion implantation at comparatively low dose, can be used to form layers of HgCdTe about one micron thick<sup>(21)</sup>. Pulsed electron beam processing will be used to restore the crystal structure of the film. This is an alternate technique to the vapor exchange method of HgCdTe fabrication.

### 3.3 ANALYSIS

The new x-ray equipment at NERC will be used extensively to characterize the films as they are deposited and processed further. Also, during the next 6 month period, some photovoltaic devices will be fashioned by NERC if the crystal quality of the HgCdTe material is good.

## REFERENCES

1. A.C. Greenwald, Semiannual report for this contract, MDA-903-79-C-0434 (March 1980), Spire Report No. SAR-80-10071-01.
2. J. Piotrowsky, Electron. Technol. (Poland) 5, 87 (1972).
3. F. Nowak, J. Piotrowsky, T. Piotrowski and A.J. Sadowski, Thin Solid Films 52, 405 (1978).
4. S.A. Semiletov, Trudy Inst. Krist. Akad. Navk SSR 11, 121 (1955); Kristallografiya 1, 306 (1956).
5. M.A. Rumsh, F.T. Novik and T.M. Zimkina, Sov. Phys. Crystallogr. 7, 711 (1963).
6. E. Suito and M. Shiojiri, K. Electron Microscopy 12, 134 (1963).
7. M. Shiojiri and E. Suito, Japan. J. Appl. Phys. 3, 314 (1964).
8. K.K. Murauyeva, I. P. Kalinkin, V.B. Aleskovsky and I.N. Anikin, Thin Solid Films 10, 355 (1972).
9. A.C. Greenwald, A.R. Kirkpatrick, R.G. Little and J.A. Minnucci, J. Appl. Phys. 50, 783 (1980).
10. A.C. Greenwald, R.G. Little and J.A. Minnucci, IEEE Trans. Nucl. Sci.: NS-26 (1), 1683 (Feb. 1979).
11. H.I. Smith, M.I.T. Lincoln Lab. No. ESD-TR-79-311, report on DARPA Contract No. F19628-78-C-0002, DARPA Order No. 3336 (30 June 1979).

12. R.F. Brebrick and A.J. Strauss, *J. Phys. Chem. Solids* 26, 989 (1965).
13. F. Bailly, L. Svob, G. Cohen-Solal and R. Triboulet, *J. Appl. Phys.* 46, 4244 (1975).
14. Final Report on Contract No. NAS-3-21276, NASA Lewis Research Center, also Spire Report No. FR-10066 (1980).
15. T.S. Sun, S.P. Buchner and N.E. Byer, *J. Vac. Sci. Technol.* 17, 1067 (1980).
16. Z.L. Liau and J.W. Mayer, *J. Vac. Sci. Technol.* 15, 1629 (1978).
17. H.H. Anderson, *J. Vac. Sci. Technol.* 16, 770 (1979).
18. Z.L. Liau, W.L. Brown, R. Hover and J.M. Poate, *Appl. Phys. Lett.* 30, 626 (1977).
19. J.E. Lewis and P.S. Ho, *J. Vac. Sci. Technol.* 16, 772 (1979).
20. M. Maenpaa, S.S. Lau, M. Von Allmen, I. Golecki, M-A. Nicolet and J.A. Minnucci, *Thin Solid Films* 67, 293 (1980).
21. Second Internal Conference on Ion Beam Modification of Materials, S.U.N.Y. at Albany (July 1980), ed. W.L. Brown and W.M. Gibson (to be published). See any paper in session on cascade implantation.